

*Photodissociation and Infrared Spectroscopy
of Uranium-Nitrogen Cation Complexes*

J. H. Marks,¹ B. M. Rittgers,¹ M. J. Van Stipdonk,² M. A. Duncan^{1*}

¹Department of Chemistry, University of Georgia, Athens, Georgia 30602, U.S.A.

²Department of Chemistry and Biochemistry, Duquesne University, Pittsburg, PA 15282, U.S.A.

*Email: maduncan@uga.edu

ABSTRACT

Laser vaporization of uranium in a pulsed supersonic expansion of nitrogen is used to produce complexes of the form $U^+(N_2)_n$ ($n = 1-8$). These ions are mass selected in a reflectron time-of-flight spectrometer and studied with visible and UV laser fixed-frequency photodissociation and with tunable infrared laser photodissociation spectroscopy. The dissociation patterns and spectroscopy of $U^+(N_2)_n$ indicate that N_2 ligands are intact molecules and that there is no insertion chemistry resulting in UN^+ or NUN^+ . Fixed frequency photodissociation at 532 and 355 nm indicate that the U^+-N_2 bond dissociation energy varies little with changing coordination. The photon energy and the number of ligands eliminated allows an estimate of the average U^+-N_2 dissociation energy of 12 kcal/mol. Infrared bands are observed for these complexes near the N-N stretch vibration via elimination of N_2 molecules. These resonances are observed to be shifted about 130 cm^{-1} to the red from the free- N_2 frequency for complexes with $n = 3-8$. Density functional theory indicates that U^+ is most stable in the sextet state in these complexes, and that N_2 molecules bind in end-on configurations. The fully coordinated complex is predicted to be $U^+(N_2)_8$, which has a cubic structure. The

vibrational frequencies predicted by theory are consistently lower than those in the experiment, independent of the isomeric structure or spin state of the complexes. Despite its failure to reproduce the infrared spectra, theory provides an average U^+-N_2 dissociation energy of 11.8 ± 0.5 kcal/mol, in good agreement with the value from the experiments.

INTRODUCTION

Actinide chemistry most often features the uranyl cation, UO_2^{2+} , because this is the prominent species present in solution.¹⁻⁵ However, uranium nitrides are also of interest as a class of ceramic materials being implemented as new nuclear energy sources.⁶⁻⁹ Uranium dinitride, UN_2 , is of particular interest because it is isoelectronic with the uranyl cation, UO_2^{2+} . However, few uranium complexes are known that contain the nitride or dinitride. Transition metal complexes with nitrogen are of course well-known in inorganic and organometallic chemistry because of the widespread importance of nitrogen activation in chemistry and biology. Transition metal neutral and ionic complexes with N_2 have been studied extensively with mass spectrometry and optical spectroscopy, as well as computational chemistry.¹⁰⁻²⁶ Actinide-nitrogen complexes are much less common, and the presence of *f* electrons is expected to have a strong influence on their bonding. In this study we employ UV-visible and infrared photodissociation measurements to investigate $U^+(N_2)_n$ complexes.

Although uranium-nitrogen bonding is uncommon, several studies have investigated these interactions. New approaches in synthetic chemistry have produced a variety of ligated uranium-nitrogen complexes.²⁷⁻³⁶ Isolated uranium-nitrides and uranium-nitrogen complexes have been studied with infrared spectroscopy of species produced in rare gas and nitrogen matrixes.³⁷⁻⁴⁵ Unfortunately, gas phase spectroscopy on uranium-nitrogen compounds is quite

limited. The UN diatomic has been studied using resonant photoionization spectroscopy.^{46,47} Bowen and coworkers recently reported the photoelectron spectrum of the uranium dinitride anion.⁴⁸ This study revealed a closed-shell electronic structure for the corresponding neutral with uranium in the +6 oxidation state, isoelectronic with the uranyl cation. The insertion of U into N₂ was found to result in a linear structure with each nitrogen triply bonded to the uranium.

The structure and bonding of actinide molecules present a range of challenges for computational chemistry. Accurately modeling the effects of relativistic electron velocity and partially occupied *f* orbitals are active areas of research. The large number of electrons poses further issues of computational cost. Relativistic Hamiltonians with all-electron treatments are preferred but are prohibitively expensive for large molecules. Fully relativistic effective core potentials (ECP) reduce computational expense and provide reasonably accurate treatment of valence electrons, where relativistic effects are small. The recently published cc-pVnZ-PP (n = D, T, Q) basis set which uses the Stuttgart/Köln fully relativistic 60 electron ECP for uranium has attracted significant interest for actinide chemistry.^{49,50} This is compatible with Dunning basis sets on non-relativistic atoms such as nitrogen. However, this and other actinide computational methods need validation through gas phase spectroscopy on uranium complexes. There are several examples of gas phase spectroscopy for small uranium oxides and uranyl ions with polyatomic ligands with corresponding computational work.⁵¹⁻⁶⁷ However, there are few examples of small ligated species that are more tractable for theory and allow its performance for coordination numbers and structures to be evaluated. In the present work, we investigate infrared spectroscopy of the U⁺(N₂)_n complexes using density functional theory (DFT) and the B3LYP functional with the cc-pVTZ-PP basis sets to predict structures and spectra of these complexes for comparison to our experiments. Previous computational work on neutral U(N₂)_n

molecules by Gagliardi and coworkers used DFT with the B3LYP functional and the SDD relativistic ECP, combined with large Pople basis sets.⁴³ These computations predicted that the fully coordinated complex contained seven nitrogen molecules bound end-on to the neutral uranium.

Infrared photodissociation (IR-PD) spectroscopy has been applied previously to transition metal cation-N₂ complexes of vanadium, niobium and rhodium.^{19,20,23} These were generally observed to have end-on bonding of nitrogen to metal, N–N stretches with strong IR activity, and N–N stretches that were shifted to the red from the frequency of isolated N₂ (2330 cm⁻¹). IR-PD has also been successful in recent investigations of uranium oxides and carbonyl complexes.^{66,67} In the case of U⁺(CO)₈, the C–O stretch vibration was observed about 60 cm⁻¹ to the red of the vibration in the isolated CO molecule (2143 cm⁻¹).⁶⁶ In the case of either CO or N₂ ligands, the well-known effects of σ donation and π back-bonding govern the charge transfer between ligand and metal, and are recognized to cause the shifts of the ligand vibrations. For transition metals, these effects involve the *d* electrons, but the role that *f* electrons may have on such interactions is not well documented. The results presented here allow a comparison of structures and spectra for the uranium-nitrogen complexes to the predictions of theory and to those of the carbonyls studied previously.

EXPERIMENTAL

Uranium cation-nitrogen complexes are produced in a pulsed supersonic expansion of 100 psi UHP nitrogen (Airgas) with laser vaporization⁶⁸ of a solid rod of depleted uranium. A Spectra Physics INDI Nd:YAG laser is used to produce up to 20 mJ/pulse at 355 nm for the vaporization. Mass separation and selection were carried out in a reflectron time-of-flight mass

spectrometer described previously.^{69,70} After mass selection, photodissociation is conducted in the turning region of the reflectron, and mass analysis of the dissociation products is determined by the transit time through a second flight tube.^{69,70} The instrumentation and methods for photodissociation are similar to those employed in our recent study of uranium oxide clusters.⁷¹ Laser radiation for fixed-frequency photodissociation at 532 and 355 nm is produced by a Spectra Physics GCR-150 Nd:YAG laser. Tunable infrared light for photodissociation is produced with a Nd:YAG-pumped infrared OPO/OPA (Laser Vision). Infrared radiation is passed through the turning region of the reflectron and retro-reflected with a concave gold folding mirror to improve the photodissociation yield.

Computational studies on uranium cation-nitrogen complexes were carried out with density functional theory and the B3LYP functional using the cc-pVTZ-PP basis set, which includes the Stuttgart/Köln fully relativistic 60 electron ECP for uranium,^{49,50} using the Gaussian16 program package.⁷² Structures containing the NUN⁺ core ion resulting from possible insertion chemistry were investigated for several of the smaller complexes. The relative energies for all proposed isomers of U⁺(N₂)_n (n = 1–8) were investigated for doublet, quartet, and sextet spin states. Isomers incorporating either side-on, or end-on bonds, or both in combination, were considered and optimized without structural constraints. Vibrational frequency and natural bond orbital (NBO) analyses were conducted on all optimized structures. A scaling factor of 0.951 was determined by predicting the frequency of the N₂ stretch at the same level of theory, and this was applied to all computed frequencies for comparison to the experimental spectra.

RESULTS AND DISCUSSION

The mass spectrum of cations produced by laser vaporization in a nitrogen expansion is shown in Figure 1. The peak for U^+ is off-scale and much larger than those for any complex or cluster ion observed, indicating a relatively inefficient clustering of molecular nitrogen with U^+ . There are small amounts of oxides and doubly charged ions, but the most prominent masses correspond to singly-charged ion-molecule complexes of the form $U^+(N_2)_n$. The mass coincidence between UN^+ and $(N_2)_9^+$ leaves some confusion as to the identity of the small peaks between each of the numbered $U^+(N_2)_n$ peaks. However, the occurrence of well-resolved $(N_2)_n^+$ peaks between U^{2+} and U^+ , where no UN^+ is possible, suggests that most of these peaks are due to pure nitrogen cluster ions. The small peak observed as a shoulder on the left side of UO^+ is UN^+ and/or $(N_2)_9^+$. Complexes of $U^{2+}(N_2)_n$ were observed in the 100 to 200 m/z range; these peaks are less intense than the N_2 cation clusters in this region. The intensities of the $U^+(N_2)_n$ peaks are greatest in the range of $n = 1-8$, with a sharp decline after this. The peaks for even values of n tend to be slightly more intense, and this is most noticeable for $n = 8$. The sharp decline of intensity for $n > 8$ strongly suggests that eight ligands complete the coordination around the U^+ ion. We saw a similar coordination of eight ligands around U^+ in our previous study of $U^+(CO)_n$ ion complexes.⁶⁶

Because the U^+ ion is expected to have a dense manifold of excited electronic states, we expected that these $U^+(N_2)_n$ complexes would absorb at visible and ultraviolet wavelengths. To investigate this, we employed fixed-frequency photodissociation measurements at the 532 and 355 nm wavelengths available from Nd:YAG laser harmonics. We found that all of these complexes absorbed and photodissociated efficiently at both wavelengths. Photodissociation mass spectra were obtained by subtracting the spectrum for each ion observed with the

photodissociation laser off from that with it on. In the resulting difference spectra, negative peaks indicate the loss of signal for the dissociated parent ion and the positive peaks indicate the resulting photofragment ions. The photodissociation mass spectra observed for $U^+(N_2)_8$ with different excitation wavelengths are shown in Figure 2. As indicated, multiple N_2 molecules are eliminated by photodissociation at each of these wavelengths. The dependence of the fragment ion peak intensity on the photodissociation laser fluence shows that the formation of U^+ responds non-linearly compared to the other fragment ions for both 532 and 355 nm photodissociation. For measurement with 355 nm, the $n = 1, 2$ and 3 fragments are observed with the same relative intensity regardless of laser power. The same is true of the $n = 3$ and 4 fragments observed at 532 nm. These fragments are therefore likely formed as the result of a single photon process. The number of ligands eliminated at each photon energy provides the average bond dissociation energy (BDE) per ligand. The elimination of 6–7 N_2 from $U^+(N_2)_8$ at 355 nm ($28,170\text{ cm}^{-1}$; 80.54 kcal/mol) indicates BDE values of 11.5–13.4 kcal/mol. The elimination of 4–5 ligands at 532 nm (18800 cm^{-1} ; 53.75 kcal/mol) likewise indicates an average BDE of 10.8–13.4 kcal/mol. These two results provide a consistent overall estimate of the N_2 binding energy of about 12 kcal/mol.

If the average U^+-N_2 BDE is in the range of 12 kcal/mol ($\sim 4200\text{ cm}^{-1}$), then single photon photodissociation should not be possible with infrared light in the region of the N–N stretch vibration (2330 cm^{-1} for the isolated molecule). Nevertheless, as shown in the lower trace of Figure 2, we do detect photodissociation with infrared excitation in this region when the laser is tuned to a resonance in the spectrum (see below). The lower trace of Figure 2 shows that 1–2 N_2 molecules can be eliminated efficiently in this way, with smaller peaks detected for the loss of 3–4 molecules. If this excitation is single photon, then the BDE must be less than about 1000

cm^{-1} (~ 3 kcal/mol). This infrared result therefore seems to be inconsistent with the results at 532 and 355 nm. However, the conditions of our infrared experiments suggest that the IR dissociation is a multiphoton process. We were unable to detect efficient dissociation with an unfocused IR laser, and therefore focused the laser to detect this signal. Laser fluence variations produced a non-linear response in fragmentation intensities for all ions studied. The infrared signals are therefore likely the result of multiphoton absorption and this result is not inconsistent with the BDE values derived earlier. If the BDE is about 12 kcal/mol, then two-photon absorption of infrared photons in this region would be sufficient to cause dissociation. Two-photon absorption is not at all unreasonable with a focused infrared laser and the strong infrared intensities for the N–N stretches, which are computed to be in the range of 1000–2000 km/mol (see below).

These photodissociation experiments reveal information about the composition of these ionic complexes. First of all, there is no evidence for the formation of any molecule containing an odd number of nitrogen atoms in the fragment ions. All the fragmentation at all wavelengths leads only to the loss of one or more N_2 molecules. The small peaks between U^+ and $n = 1$ in Figure 2 were determined to result from photodissociation to form U^+ and $\text{U}^+(\text{N}_2)$ by nearby masses not fully attenuated by the mass selector. This suggests that there are no $\text{UN}^+(\text{N}_2)_n$ species present which might result from reactions of U^+ with N_2 under the energetic plasma conditions. There also appear to be no ions of the form $\text{NUN}^+(\text{N}_2)_n$ which might result from insertion reactions. This is evident because the photodissociation experiments at 532 and 355 nm all terminate at the atomic U^+ ion rather than NUN^+ . Neutral NUN is isoelectronic to UO_2^{2+} and therefore expected to be strongly bound, and NUN^+ should also have strong covalent bonding. If NUN^+ were present in these ion clusters, it would likely survive as a terminal ion,

but we do not see this. Bowen and coworkers⁴⁸ observed negative ions of the form NUN^- and Andrews and coworkers⁴³⁻⁴⁵ detected similar neutral reaction products in matrix isolation experiments. However, this insertion product is not seen in our dissociation experiments, and is apparently not formed in our source. It is conceivable that NUN^+ ions are formed, but that they do not absorb and dissociate at either of the 532 or 355 nm wavelengths. We do not have any information about the excited states of NUN^+ , and cannot be sure that it would absorb at these wavelengths. On the other hand, we have used high-power laser conditions that usually dissociate ions even if they do not absorb strongly. Therefore, although we cannot absolutely prove that NUN^+ ions are not present, the simplest interpretation of our fragmentation data is that these ions represent $\text{U}^+(\text{N}_2)_n$ atomic ion-molecular complexes.

As shown below, infrared excitation leads to photodissociation of these ions with resonances in the region near the N–N stretch of molecular nitrogen (2330 cm^{-1}). Photodissociation mass spectra for $\text{U}^+(\text{N}_2)_n$ for $n = 3-8$ were obtained at the peak absorption found for each complex. The $n = 1$ and 2 ions did not dissociate under these conditions, suggesting that they have relatively high dissociation energies. Other ions dissociated by elimination of one or more N_2 molecules, as shown in Figure 2 for the $n = 8$ species. Figure S5 in the Supporting Information file shows the fragmentation patterns for the $n = 3-8$ ions. Those ions larger than $n = 4$ all dissociate via a sequence of N_2 losses terminating at the $n = 4$ ion. This suggests that the $n = 4$ complex possesses some additional stability beyond that of larger complexes. This complex would possess a half-filled inner coordination if the fully coordinated complex is $n = 8$ as indicated by the mass spectrum in Figure 1.

The infrared photodissociation (IR-PD) spectra of $\text{U}^+(\text{N}_2)_n$ ($n = 3-8$) are shown in Figure 3. Because fragmentation was not detected with infrared for the $n = 1$ or 2 complexes, no spectra

were obtained for those ions. We attempted to obtain spectra for these ions via rare gas tagging with argon, but were unable to produce sufficient quantities of the tagged ions. As shown in the figure, the $n = 3-8$ ions all have resonances near that of the N–N stretch of the isolated N_2 molecule at 2330 cm^{-1} , whose position is marked with the vertical dashed red line. The $n = 3$ and 4 complexes have three and two bands each, whereas all the larger complexes have a single resonance. The resonances for the $n = 5, 6, 7$ complexes are broad, suggesting the possibility of overlapping bands for multiple isomers, whereas that for the $n = 8$ complex is particularly sharp. The most prominent bands for all of these complexes appear at frequencies about 100 cm^{-1} lower than the free- N_2 stretch; weaker bands for the $n = 3$ and 4 complexes appear at frequencies higher than the N_2 stretch. The $n = 8$ complex is the largest ion produced in the mass spectrometer with sufficient intensity to allow a spectrum to be measured.

The shift of the N–N vibrations to lower frequency upon binding to a metal ion has been seen previously for transition metal ion-nitrogen complexes,^{19,20,23} and for neutral $U(N_2)_n$, $UN(N_2)_n$ and $NUN(N_2)_n$ complexes in matrix isolation experiments.⁴⁴ This red shift is explained using the Dewar-Chatt-Duncanson model of metal-ligand charge transfer, and is analogous to the shifts seen for many metal-carbonyl complexes.⁷³ In the case of metal carbonyls, there is a competition between ligand→metal σ -donation, which leads to higher frequencies, and metal→ligand π back-bonding, which leads to lower frequencies. In the case of metal-nitrogen complexes, both effects tend to lower the N–N stretch frequency, as seen here. These effects have been seen for transition metal ion-nitrogen complexes,^{19,20,23} and for the $U^+(CO)_n$ complexes,⁶⁶ but this is the first example of an actinide cation-nitrogen system, where the f orbitals are involved. The specific values of these red shifts are expected to vary with the structure and electronic state of the complexes, as discussed below.

Computational chemistry at the B3LYP/cc-pVTZ-PP level was used to predict the structures, electronic states, and vibrational frequencies of $U^+(N_2)_n$ for $n = 1-8$, and $NUN^+(N_2)_{n-1}$ for $n = 1-7$ for comparison to the IR-PD spectra. Doublet, quartet, and sextet electronic states were investigated for different structural isomers of $U^+(N_2)_n$. A full account of this computational work is provided in the Supporting Information file. The sextet electronic states are invariably the lowest in energy by about 9 kcal/mol, followed by the quartets and then the doublets, which are usually 12 to 20 kcal/mol higher in energy than the sextet. It should be noted that DFT tends to over-stabilize high spin states, although this effect is unlikely to produce errors on the order of 9 kcal/mol. We also recognize that spin is not a good quantum number for a heavy element such as uranium, but this provides a convenient framework for these computations. In the case of the $NUN^+(N_2)_{n-1}$ complexes, the doublets are lowest in energy. This is because of the closed-shell nature of NUN, which consists of U in the +6 oxidation state with triple bonding to two axial nitrogen atoms. Formation of NUN^+ in higher spin states would correspond to ionization of excited states of NUN, because a closed shell neutral can only produce a doublet upon ionization. Ionization of this species requires the removal of an electron from a core orbital of uranium. The ionization potential (IP) of NUN is predicted to be 8.87 eV, which is about 3 eV higher than that of uranium atom (6.19 eV).⁵⁰ This IP difference outweighs the added stability of the covalent bond energy, and the NUN^+ doublet is predicted to lie 11.9 kcal/mol above the energy of $U^+(N_2)$. As indicated in Table 1, the structures of $NUN^+(N_2)_{n-1}$ complexes for $n = 2$ or 3 are also predicted to be less stable (+9.4 and +8.3 kcal/mol) than the non-inserted isomers, and the energy difference compared to $U^+(N_2)_n$ structures becomes even greater in the larger clusters.

The structures predicted for the $U^+(N_2)_{1-8}$ complexes are shown in Figure 4. The relative energies of different isomers and spin states are presented in Table 1. The isomers shown here are those predicted to be most stable for each value of n , and they all have the nitrogen molecules bonded in end-on configurations. Similar end-on ligand configurations were reported previously for neutral $U(N_2)_n$, $UN(N_2)_n$ and $NUN(N_2)_n$ complexes in matrix isolation experiments.^{43,44} Structures with side-on or a mixture of end-on and side-on bonding were also investigated, as described in the Supporting Information. The $n = 4$ and 5 complexes are predicted to have trigonal pyramidal and trigonal bipyramidal coordination, respectively. The $n = 6$ and 7 complexes have asymmetric coordination, with some ligands in positions resembling those in the cubic structure found for $n = 8$, but with vacancies in the coordination. The $n = 8$ complex is predicted to have cubic symmetry in the T_d point group. The metal– N_2 bonding distances vary in different structures, but are all close to 2.5 \AA . The end-on bonding in these structures results in a slight elongation of the N_2 bonds compared to those in the isolated molecule. This elongation varies with bonding structures and positions between 0.033 \AA in the 1a sextet and 0.008 \AA in the 8a sextet.

The binding energies of the nitrogen molecules in these structures are predicted to be in the range of $9\text{--}13 \text{ kcal/mol}$ (Table 1); the average BDE over different cluster sizes is $11.8 \pm 0.5 \text{ kcal/mol}$. As discussed previously for metal-nitrogen ions, this is the range expected for bonding that is primarily electrostatic (charge-quadrupole) in nature.^{19,20,23} These calculated bond energies are consistent with the average value of 12 kcal/mol estimated earlier from the photodissociation experiments. The highest bond energy predicted is that for isomer 4a in its sextet state (14.0 kcal/mol). Consistent with this, the $n = 4$ species also shows a tendency to survive more in the photodissociation experiments (Figure 2).

The measured spectrum of $U^+(N_2)_3$ is shown in Figure 5 together with the spectra predicted by theory for several possible isomers and spin states. The complete details of the structures are provided in the Supporting Information. As shown, no spectrum predicted for any single isomer or spin state matches the experiment. The spectrum for the lowest energy isomer 3a does not match the spectrum very well in terms of band positions, but it has the pattern of one strong band at lower frequency and another weaker one at higher frequency which is somewhat like that of the more intense bands in the experiment. The structures of the 3a species in different spin states are similar, but the computed relative energies increase with lower spin states. The spectra predicted for isomer 3a in its sextet, quartet, and doublet states have different patterns, but all of their bands appear at frequencies much lower than the bands in the experimental spectrum. The 3b and 3c sextets both include one and two N_2 ligands, respectively, binding side-on, with relative energies of +3.2 kcal/mol for 3b and +4.1 kcal/mol for 3c. These structures both have bands predicted within 20 cm^{-1} of the main experimental peak at 2245 cm^{-1} peak, but each also has bands predicted near 1880 cm^{-1} from the stretching of the side-on bound N_2 , where no signal is observed in the experiment. Isomer 3d has an NUN^+ core ion in its doublet state, which was investigated to see if there was an evidence for insertion chemistry. The nitride stretch vibrations from this core ion are predicted below 1000 cm^{-1} , which is well below the dissociation energy and in a region where the available laser power is far too low for multiphoton dissociation. However, the stretches of the additional N_2 ligands for this possible isomer could be detected. This structure is predicted to produce nearly no red shift of the N_2 stretch in the end-on ligands, with a band at 2326 cm^{-1} , in nearly the same position as the free N_2 stretch at 2330 cm^{-1} . This is higher than the main experimental band, but lower than the broad high frequency band. The formation of the NUN^+ structure is expected to be energetically

unfavorable, decreasing the stability of the complex by 8.3 kcal/mol. However, the vibration at 2336 cm^{-1} predicted for isomer 3d is the closest of any band for any isomer to the experimental peak at 2394 cm^{-1} . This spectral evidence suggests that an NUN^+ ion might be present at low concentration, but this contradicts our photodissociation patterns at 355 and 532 nm, which found no evidence for a surviving ion with this composition. Because of these conflicting observations, it is not clear at all how to assign the $\text{U}^+(\text{N}_2)_3$ spectrum. It is most likely to arise from the presence of more than one structural isomer or spin state, but none of the spectra match the experiment very well. We must therefore conclude that either the computed energies of different isomers and spin states, or the vibrational patterns predicted for them, are in error.

The experimental spectrum of $\text{U}^+(\text{N}_2)_4$ is shown in Figure 6 together with simulated spectra of isomers 4a–d, which have various end-on and side-on structures with N_2 ligands attached to a U^+ core ion in its sextet spin state. Isomer 4f is also included, which is the lowest energy structure containing an NUN^+ core ion. There are multiple ways to arrange the end-on N_2 ligands to produce isomers such as 4a and 4c, and side-on binding produces additional isomers. The 4a and 4c isomers are both predicted to have intense absorptions which might be attributed to the observed 2232 cm^{-1} peak. Isomer 4c is only slightly distorted from a square-planar configuration, which would have only a single band corresponding to degenerate vibrations. However, as was the case with $\text{U}^+(\text{N}_2)_3$, these vibrations are all predicted to be too far to the red of the measured absorption. The peak predicted at 1978 cm^{-1} for isomer 4a is not evident in the experimental data, as only baseline is observed to the red of the 2232 cm^{-1} peak. The 4d isomer predicts the N_2 ligands with side-on binding to vibrate in the region of 1900 cm^{-1} where again there is no signal. In the spectra for both $\text{U}^+(\text{N}_2)_3$ and $\text{U}^+(\text{N}_2)_4$ the N_2 in an end-on bond is expected to have a resonance over 100 cm^{-1} to the red of the observed peak, and the side-on

binding N_2 is expected to have this over 300 cm^{-1} to the red of the observed peak. It may be that these calculations overestimate the effect of the uranium cation on the end-on nitrogen. If this is the case, then it is plausible that isomer 4c is the structure present, and its two peaks are simply not resolved. Furthermore, none of these spectra predict any vibration which could explain the peak at 2371 cm^{-1} . This could be a combination band of the N_2 stretch with a low-frequency U^+-N_2 stretch, which is predicted in about the right frequency range, but whose IR activity in such a combination would not be predicted by the present harmonic theory. Alternatively, this peak could originate from the presence of a small amount of $\text{NUN}^+(\text{N}_2)_3$, as noted above for the $n = 3$ complex. As described there, an $\text{NUN}^+(\text{N}_2)_2$ structure is predicted to be less stable, but produces the highest frequency N_2 stretch.

Figure 7 shows the infrared spectrum of $\text{U}^+(\text{N}_2)_6$ compared to the spectra for different structural isomers. The spectrum has a single relatively broad band at 2198 cm^{-1} . The trace of a higher frequency band seen in the smaller clusters (e.g., 2371 cm^{-1} for the $n = 4$ species) is no longer detected for this cluster size. As we found for the smaller complexes, the spectra of sextet, quartet and doublet species having the same structures are very similar, and so we show only the spectra for the lowest energy sextet structures. Structures 6a and 6b have a U^+ core ion with all ligands bound in end-on configurations, in structures close to an octahedron. As seen for the smaller clusters, the N–N stretches predicted for these structures are lower than the main band in the experiment. However, the discrepancy is less than it was for the smaller clusters, and the predicted bands form a close multiplet that might not be resolved in the experiment. The multiplet splittings result from the small displacements from the octahedral structure; if the structure were octahedral, the high symmetry would result in a degenerate vibration with a single band. Structure 6d is the lowest in energy of several species having side-on bonding to N_2

ligands. As in the $n = 3$ and 4 species, such ligands are again predicted to have strong vibrations at low frequencies, where no signal is detected. Finally, isomer 6g has the NUN^+ core ion. This species again has a single high frequency vibration for its N_2 ligands, but its computed energy is even higher relative to other structures, and no signal is detected in this region for this cluster.

The experimental spectrum of $\text{U}^+(\text{N}_2)_8$ is shown in Figure 8 with spectra predicted by theory for the three lowest energy isomers. The most stable isomer 8a contains only end-on bonded ligands in a highly symmetric cubic structure, whereas isomers 8b and 8c each contain two N_2 ligands with side-on bonding and are predicted to be considerably less stable. Because of the filled coordination of these complexes, side-on binding introduces steric strain not evident in the smaller complexes. Rotation of two ligands from the end-on configuration of isomer 8a to side-on configuration bonds results in increases in energy of 18.5 and 18.7 kcal/mol for isomers 8b and 8c. By comparison, rotation of two ligands in $\text{U}^+(\text{N}_2)_4$ increased the energy by only 5.2 kcal/mol (isomer 4d; Figure 6). This effect is attributed entirely to the steric crowding of ligands about the uranium ion. This crowding also results in a change in coordination geometry from the cubic structure of isomer 8a to the square antiprism configurations for isomers 8b and 8c. A similar square antiprism structure was found previously for the coordination of $\text{U}^+(\text{CO})_8$, although in that complex all the carbonyl ligands were predicted to bind in end-on U^+-CO configurations.⁶⁶ Unlike the patterns seen for the smaller clusters, the experimental and predicted spectra here seem to be in better agreement. The peak predicted for isomer 8a at 2184 cm^{-1} is only 28 cm^{-1} lower than the single sharp experimental band at 2212 cm^{-1} . No other isomer of this complex is predicted to produce a spectrum consisting of a single peak. The 8a isomer optimized to cubic coordination without any symmetry constraints and is expected to represent the fully coordinated complex. The spectra for other low energy isomers with ligands

in side-on configurations have additional structure both above and below the experimental band, and can be safely ruled out. The $U^+(N_2)_8$ complex can therefore be concluded to have the highly-symmetric cubic structure. According to the strong preference for this species in the mass spectrum, this can be concluded to be the filled coordination for nitrogen molecules around the U^+ ion. This cubic structure for $U^+(N_2)_8$ contrasts to the square antiprism found previously for $U^+(CO)_8$,⁶⁶ but the eight-fold coordination for both ligands makes sense. In both cases, the number of valence electrons (5 on the U^+ plus 16 from the ligands = 21) is close to the closed-shell count of 22 expected for stable actinide complexes.¹⁻⁴

As shown and discussed here, the overall agreement between theory and experiment for the vibrational patterns of these $U^+(N_2)_n$ complexes is disappointing. Figures 5–8 here, and those for $U^+(N_2)_5$ and $U^+(N_2)_7$ in the Supporting Information (Figures S54–56, S77–78), show that the agreement is worse for the small clusters, which have partially filled coordination, and progressively better for the larger ones. It is difficult for the small clusters to find any predicted vibrational pattern that matches the experiment, whereas the spectra predicted for $U^+(N_2)_7$ and $U^+(N_2)_8$ are in reasonable agreement with the experiment. It is not clear what causes the deficiencies of theory, nor why it should be worse for the smaller complexes. Any of the approximations that are used to make actinide theory computationally affordable may be the issue. This includes the use of an ECP with the implicit neglect of core-valence correlation and relativistic effects on valence electrons. The electronic states of U^+ are likely better represented with multireference wavefunctions. Strong field spin-orbit in uranium causes further coupling between states of different multiplicity. Unfortunately, multireference calculations and appropriate treatment of spin-orbit coupling are not affordable in complexes containing more than two or three atoms in addition to uranium. To further investigate this issue, and to validate

the level of theory used here, we have applied this method to the $U^+(CO)_8$ and $UO_2^+(CO)_5$ complexes studied previously by our group.⁶⁶ As shown in Figures S87 and S88 in the Supporting Information, the present level of theory performs significantly better than the DFT/PBE method with the SDD pseudopotential employed previously,⁶⁶ and reproduces both the direction (relative to the CO stretch of the isolated molecule) and the magnitude of the shifts for carbonyl stretch frequencies of these complexes. We find a similar result for the spectra measured previously for UO_4^+ and UO_6^+ ions,⁶⁷ as shown in Figures S89 and S90. However, these carbonyl and oxo ions are all fully coordinated like the $U^+(N_2)_8$ complex here. We are unable to investigate any other partially coordinated complexes because of the lack of suitable experimental data. Future experiments will continue this line of work, examining under-coordinated species of uranium and its oxide ions with a variety of small ligands.

Although the spectra predicted by theory are not definitive, the patterns produced are useful in identifying the most likely structures present in the experiment. Except for the $n = 3$ complex, the experimental spectra of all the cluster sizes are dominated by one main resonance. This implies that the structures have high symmetry. If there are distortions from these structures, the vibrations that are degenerate at high symmetry begin to separate and split apart gradually. The broader widths of the spectra for the $n = 3, 5, 6, 7$ complexes suggest that their structures may deviate slightly from high-symmetry, producing some width from un-resolved resonances. The bands for the $n = 4$ and 8 complexes are sharper, suggesting higher-symmetry structures and/or fewer contributing isomers. Except for the $n = 3$ complex, theory for each of the different cluster sizes has at least one isomer at low energy that has a high-symmetry structure, or one close to this, with either a single main band or a few closely-spaced bands. For the $n = 4$ complex, isomer 4c has a structure near square-planar, with two closely-spaced bands.

Isomer 5a in its sextet and doublet states (Figure S54) has a structure near trigonal pyramidal, with two closely-spaced bands. Isomer 6a and 6b has a structure close to octahedral in several spin states. Isomer 7a (Figure S77) has a high-symmetry structure, with nearly a single band in each of its spin states, and isomer 8a is the cubic structure with a single predicted band, as noted earlier. If we admit that theory might miss these exact frequencies, each of these high-symmetry structures is plausible and provides a reasonable assignment for our spectra. It is clear, however, that we cannot make any firm conclusions about spin states. There are really no examples where low-lying structures have a distinctive pattern for different spins that can be assigned to the experimental spectrum. Except for the $n = 5$ species (Figure S54), the different spin states for each isomer have very similar band patterns. Therefore, although the data for these uranium-nitrogen ions are not definitive for the smaller clusters, our results suggest the most likely structures for these species, and it provides more clear conclusions about the structures of the larger clusters.

CONCLUSIONS

Laser vaporization and supersonic expansions were used to produce small $U^+(N_2)_n$ complexes. These complexes were mass selected and studied via fixed-frequency photodissociation at visible and UV wavelengths, and with tunable laser photodissociation spectroscopy in the infrared. Fixed-frequency photodissociation shows that molecular nitrogen ligands bound to uranium ion are readily eliminated down to a terminal fragment of U^+ . This indicates that no inserted NUN^+ ions are present at the core of these clusters. The ratio of photon energy to ligands eliminated across multiple complexes provides an estimate of the average U^+-N_2 bond dissociation energy of 12 kcal/mol. Infrared photodissociation spectra show that the

N–N stretch becomes IR-active and shifts 100 to 130 cm^{-1} to lower frequency because of the interaction with the uranium cation. Computations at the B3LYP/cc–pVTZ–PP level are used to investigate the structures and infrared spectra of the $\text{U}^+(\text{N}_2)_n$ ions. These computations find multiple isomers for the small clusters, with close energetics and similar spectra. Bond dissociation energies are predicted to be in the range of 10–13 kcal/mol, in agreement with the experimental estimate. The spectra predicted for the lower energy isomers contain bands that are shifted to lower frequencies than the isolated molecule vibration, with only small variations in patterns for different spin states. However, the red shifts are consistently greater than those observed experimentally. The deviation between predicted and observed frequencies decreases as cluster size increases, and the coordination becomes more complete, and the agreement between theory and experiment is eventually quite good for the $\text{U}^+(\text{N}_2)_7$ and $\text{U}^+(\text{N}_2)_8$ complexes. Theory predicts that the sextet $\text{U}^+(\text{N}_2)_8$ is a fully coordinated ion with eight N_2 ligands bound in end-on configurations with a cubic structure. These actinide ion complexes provide ongoing challenges, with fundamental questions remaining about structures, spectra and spin states, but infrared spectroscopy experiments like these provide perhaps the most detailed experimental data addressing these issues.

Author Information

Corresponding author: Email: maduncan@uga.edu

ORCID: 0000-0003-4836-106x

Acknowledgments

We acknowledge generous support for this work from the U. S. Department of Energy through grant no. DE-SC0018835.

Supporting Information Available: The full citation for reference 72 and the details of the DFT computations done in support of the spectroscopy presented here, including the structures, energetics, and simulated vibrational spectra for each of the complexes considered. This material is available free of charge via the Internet at <http://pubs.acs.org>.

REFERENCES

1. Katz, J. J.; Seaborg, G. T.; Morss, L. R. *The Chemistry of the Actinide Elements*, 2nd ed., Chapman and Hall: London, **1986**.
2. Aspinall, H. C. *Chemistry of the f-Block Elements*, Gordon and Breach: Amsterdam, **2001**.
3. Cotton, S. *Lanthanide and Actinide Chemistry*, John Wiley & Sons, Ltd.: Chichester, **2006**.
4. Konings, R. J. M.; Morss, L. R.; Fuger, J. *The Chemistry of the Actinide and Transactinide Elements*, 3rd ed., edited by L. R. Morss, N. M. Edelstein, and J. Fuger Springer: Dordrecht, **2006**.
5. Maher, K.; Bargar, J. R.; Brown, G. E., Jr. Environmental Speciation of Actinides. *Inorg. Chem.* **2013**, *52*, 3510–3532.
6. Matthews, R. B.; Chidester, K. M.; Hoth, C. W.; Mason, R. E.; Petty, R. L. Fabrication and Testing of Uranium Nitride Fuel for Space Power Reactors. *J. Nucl. Mater.* **1988**, *151*, 345–356.
7. Rogozkin, B. D.; Stepennova, N. M.; Bergman, G. A.; Proshkin, A. A. Thermochemical Stability, Radiation Testing, Fabrication, and Reprocessing of Mononitride Fuel. *Atomic Energy* **2003**, *95*, 835–844.
8. Streit, M.; Ingold, F. Nitrides as a Nuclear Fuel Option. *J. Eur. Ceram. Soc.* **2005**, *25*, 2687–2692.
9. Allen, D. J.; Blair, S. R.; Millett, M. G.; Nelson, M. E. Evaluation of Non-Oxide Fuel for Fission-Based Nuclear Reactors on Spacecraft. *Nucl. Technol.* **2019**, *205*, 755–765.

10. Khan, F. A.; Steele, D. L.; Armentrout, P. B. Ligand Effects in Organometallic Thermochemistry: The Sequential Bond Energies of $\text{Ni}(\text{CO})_x^+$ and $\text{Ni}(\text{N}_2)_x^+$ ($x = 1-4$) and $\text{Ni}(\text{NO})_x^+$ ($x = 1-3$). *J. Phys. Chem.* **1995**, *99*, 7819–7828.
11. Tjelta, B. L.; Armentrout, P. B. Gas-Phase Metal Ion Ligation: Collision-Induced Dissociation of $\text{Fe}(\text{N}_2)_x^+$ ($x = 1-5$) and $\text{Fe}(\text{CH}_2\text{O})_x^+$ ($x = 1-4$). *J. Phys. Chem. A* **1997**, *101*, 2064–2073.
12. Tjelta, B. L.; Walter, D.; Armentrout, P. B. Determination of Weak Fe^+ -L Bond Energies (L = Ar, Kr, Xe, N_2 , and CO_2) by Ligand Exchange Reactions and Collision-Induced Dissociation. *Int. J. Mass. Spectrom.* **2001**, *204*, 7–21.
13. Asher, R. L.; Buthelezi, B.; Brucat, P. J. Optical Excitation of $\text{Co}^+\cdot\text{N}_2$. *J. Phys. Chem.* **1995**, *99*, 1068–1072.
14. Heinemann, C.; Schwarz, J.; Schwarz, H. Ground state of $\text{Co}(\text{N}_2)^+$. *J. Phys. Chem.* **1996**, *100*, 6088–6092.
15. Bauschlicher, C. W., Jr.; Petterson, L. M.; Siegbahn, P. E. M. The Bonding in FeN_2 , FeCO , and Fe_2N_2 : Model Systems for Side-On Bonding of CO and N_2 . *J. Chem. Phys.* **1987**, *87*, 2129–2137.
16. Duarte, A. D.; Salahub, D. R.; Haslett, T.; Moskovits, M. $\text{Fe}(\text{N}_2)_n$ ($n = 1-5$): Structure, Bonding, and Vibrations from Density Functional Theory. *Inorg. Chem.* **1999**, *38*, 3895–3903.
17. Andrews, L.; Bare, W. D.; Chertihin, G. V. Reactions of Laser-Ablated V, Cr, and Mn Atoms with Nitrogen Atoms and Molecules. Infrared Spectra and Density Functional Calculations on Metal Nitrides and Dinitride Complexes. *J. Phys. Chem. A* **1997**, *101*, 8417–8427.

18. Parrish, S. H.; Van Zee, R. J.; Weltner, W., Jr. Vanadium and Niobium Hexadinitrogen and Hexacarbonyl Complexes: Electron-Spin-Resonance Spectra at 4 K. *J. Phys. Chem. A* **1999**, *103*, 1025–1028.
19. Pillai, E. D.; Jaeger, T. D.; Duncan, M. A. IR Spectroscopy and Density Functional Theory of Small $V^+(N_2)_n$ Complexes. *J. Phys. Chem. A* **2005**, *129*, 3521–3526.
20. Pillai, E. D.; Jaeger, T. D.; Duncan, M. A. IR Spectroscopy of $Nb^+(N_2)_n$ Complexes: Coordination, Structures, and Spin States. *J. Am. Chem. Soc.* **2007**, *129*, 2297–2307.
21. Lu, Z.-H.; Jiang, L.; Xu, Q. Reactions of Laser-Ablated Nb and Ta Atoms with N_2 : Experimental and Theoretical Study of $M(NN)_x$ ($M = Nb, Ta$; $x = 1-4$) in Solid Neon. *J. Phys. Chem. A* **2010**, *114*, 6837–6842.
22. Lu, Z.-H.; Jiang, L.; Xu, Q. A Combined Experimental and Theoretical Study of Iron Dinitrogen Complexes: $Fe(N_2)$, $Fe(NN)_x$ ($x = 1-5$), and $Fe(NN)_3^-$. *J. Phys. Chem. A* **2010**, *114*, 2157–2163.
23. Brathwaite, A. D.; Abbott-Lyon, H. L.; Duncan, M. A. Distinctive Coordination of CO vs N_2 to Rhodium Cations: An Infrared and Computational Study. *J. Phys. Chem. A* **2016**, *120*, 7659–7670.
24. Xie, H.; Shi, L.; Xing, X.; Tang, Z. Infrared Photodissociation Spectroscopy of $M(N_2)_n^+$ ($M = Y, La, Ce$; $n = 7-8$) in the Gas Phase. *Phys. Chem. Chem. Phys.* **2016**, *18*, 4444–4450.
25. Ding, K.; Xu, H.; Yang, Y.; Li, T.; Chen, Z.; Ge, Z.; Zhu, W.; Zheng, W. Mass Spectrometry and Theoretical Investigation of VN_n^+ ($n = 8, 9, \text{ and } 10$) Clusters. *J. Phys. Chem. A* **2018**, *122*, 4687–4695.

26. Yoo, H.-W.; Choi, C.; Cho, S. G.; Jung, Y.; Choi, M. Y. Infrared Spectroscopy and Density Functional Calculations on Titanium-Dinitrogen Complexes. *Chem. Phys. Lett.* **2018**, *698*, 163–170.
27. Evans, W. J.; Kozimor, S. A.; Ziller, J. W. Molecular Octa-Uranium Rings with Alternating Nitride and Azide Bridges. *Science* **2005**, *309*, 1835–1838.
28. Thomson, R. K.; Cantat, T.; Scott, B. L.; Morris, D. E.; Batista, E. R.; Kiplinger, J. L. Uranium Azide Photolysis Results in C–H Bond Activation and Provides Evidence for a Terminal Uranium Nitride. *Nature Chem.* **2010**, *2*, 723–729.
29. King, D. M.; Tuna, F.; McInnes, E. J. L.; McMaster, J.; Lewis, W.; Blake, A. J.; Liddle, S. T. Synthesis and Structure of a Terminal Uranium Nitride Complex. *Science* **2012**, *337*, 717–720.
30. King, D. M.; Tuna, F.; McInnes, E. J. L.; McMaster, J.; Lewis, W.; Blake, A. J.; Liddle, S. T. Isolation and Characterization of Uranium(VI)-Nitride Triple Bond. *Nature Chem.* **2013**, *5*, 482–488.
31. Hayton, T. W. Recent Developments in Actinide-Ligand Multiple Bonding. *Chem. Commun.* **2013**, *49*, 2956–2973
32. King, D. M.; Liddle, S. T. Progress in Molecular Uranium-Nitride Chemistry. *Coord. Chem. Rev.* **2014**, *2*, 266–267.
33. Liddle, S. T. The Renaissance of Non-Aqueous Uranium Chemistry. *Angew. Chem. Int. Ed.* **2015**, *54*, 8604–8641.
34. Cleaves, P. A.; Kefalidis, C. E.; Gardner, B. M.; Tuna, F.; McInnes, E. J. L.; Lewis, W.; Maron, L.; Liddle, S. T. Terminal Uranium(V/VI) Nitride Activation of Carbon Dioxide

- and Carbon Disulfide: Factors Governing Diverse and Well-Defined Cleavage and Redox Reactions. *Chem. Eur. J.* **2017**, *23*, 2950–2959.
35. Rudel, S. S.; Deubner, H. L.; Müller, M.; Karttunen, A. J.; Kraus, F. Complexes Featuring a Linear $[N=U\equiv N]$ Core Isoelectronic to the Uranyl Cation. *Nature Chem.* **2020**, *12*, 962–967.
36. Fortier, S.; Wu, G.; Hayton, T. W. Synthesis of a Nitrido-Substituted Analogue of the Uranyl Ion, $[N=U=O]^+$. *J. Am. Chem. Soc.* **2010**, *132*, 6888–6889.
37. Green, D. W.; Reedy, G. T. The Identification of UN in Ar Matrices. *J. Chem. Phys.* **1976**, *65*, 2921–2922.
38. Hunt, R. D.; Yustein, J. T.; Andrews, L. Matrix Infrared Spectra of NUN Formed by the Insertion of Uranium Atoms into Molecular Nitrogen. *J. Chem. Phys.* **1993**, *98*, 6070–6074.
39. Kushto, G. P.; Souter, P. F.; Andrews, L.; Neurock, M. A. Matrix Isolation FT-IR and Quasirelativistic Density Functional Theory Investigation of the Reaction Products of Laser-Ablated Uranium Atoms with NO, NO₂ and N₂O. *J. Chem. Phys.* **1997**, *106*, 5894–5903.
40. Zhou, M.; Andrews, L. Infrared Spectra and Pseudopotential Calculations for NUO⁺, NUO, and NThO in Solid Neon. *J. Chem. Phys.* **1999**, *111*, 11044–11049.
41. Andrews, L.; Wang, X.; Lindh, R.; Roos, B. O.; Marsden, C. J. Simple NUF₃ and PUF₃ Molecules with Triple Bonds to Uranium. *Angew. Chem. Int. Ed.* **2008**, *47*, 5366–5370.
42. Wang, X., Andrews, L., Vlasisavljevich, B.; Gagliardi, L. Combined Triple and Double Bonds to Uranium: The $N\equiv U=N-H$ Uranimine Nitride Molecule Prepared in Solid Argon. *Inorg. Chem.* **2011**, *50*, 3826–3831.

43. Andrews, L.; Wang, X.; Gong, Y.; Vlaisavljevich, B.; Gagliardi, L. Infrared Spectra and Electronic Structure Calculations for the NUN(NN)₁₋₅ and NU(NN)₁₋₆ Complexes in Solid Argon. *Inorg. Chem.* **2013**, *52*, 9989–9993.
44. Andrews, L.; Wang, X.; Gong, Y.; Kushto, G. P.; Vlaisavljevich, B.; Gagliardi, L. Infrared Spectra and Electronic Structure Calculations for NN Complexes with U, UN and NUN in Solid Argon, Neon and Nitrogen. *J. Phys. Chem. A* **2014**, *118*, 5289–5303.
45. Sankaran, K.; Sundararajan, K.; Viswanathan, K. S. Matrix Isolation Infrared Studies of the Reactions of Laser-Ablated Uranium with N₂: Reactions Beyond Insertion into N₂. *J. Phys. Chem. A* **2001**, *105*, 3995–4001.
46. Matthew, D. J.; Morse, M. D. Resonant Two-Photon Photoionization Spectroscopy of Jet-Cooled UN: Determination of the Ground State. *J. Chem. Phys.* **2013**, *138*, 184303.
47. Battey, S. R.; Bross, D. H.; Peterson, K. A.; Persinger, T. D.; VanCundy, R. A.; Heaven, M. C. Spectroscopic and Theoretical Studies of UN and UN⁺. *J. Chem. Phys.* **2020**, *152*, 094302.
48. Gaoziang, L.; Zhang, C.; Ciborowski, S. M.; Asthana, A.; Cheng, L.; Bowen, K. H. Mapping the Electronic Structure of the Uranium(VI) Dinitride Molecule, UN₂. *J. Phys. Chem. A* **2020**, *124*, 6486–6492.
49. Peterson, K. A. Correlation Consistent Basis Sets for Actinides. I. The Thorium and Uranium Atoms. *J. Chem. Phys.* **2015**, *142*, 074105.
50. Dolg, M.; Cao, X. Accurate Relativistic Small-Core Pseudopotentials for Actinides. Energy Adjustments for Uranium and First Applications to Uranium Hydride. *J. Phys. Chem. A* **2009**, *113*, 12573–12581.

51. Gibson, J. K. Gas-Phase Chemistry of Actinide Ions: Probing the Distinctive Character of the *5f* Elements. *Int. J. Mass Spectrom.* **2002**, *214*, 1–21.
52. Heaven, M. C.; Nicolai, J.-P.; Riley, S. J.; Parks, E. K. Rotationally Resolved Electronic Spectra for Uranium Monoxide. *Chem. Phys. Lett.* **1985**, *119*, 229–233.
53. Allen, G. C.; Holmes, N. R. Mixed-Valency Behavior in Some Uranium-Oxides Studies by X-Ray Photoelectron Spectroscopy. *Can. J. Spectros.* **1993**, *38*, 124–130.
54. Kaledin, L. A.; McCord, J. E.; Heaven, M. C. Laser Spectroscopy of UO: Characterization and Assignment of States in the 0 to 3 eV Range, with a Comparison to the Electronic Structure of ThO. *J. Mol. Spec.* **1994**, *164*, 27–65.
55. Kaledin, L. A.; Heaven, M. C. Electronic Spectroscopy of UO. *J. Mol. Spec.* **1997**, *185*, 1–7.
56. Lue, C. J.; Jin, J.; Ortiz, M. J.; Rienstra-Kiracofe, J. C.; Heaven, M. C. Electronic Spectroscopy of UO₂ Isolated in a Solid Ar Matrix. *J. Am. Chem. Soc.* **2004**, *126*, 1812–1815.
57. Han, J.; Goncharov, V.; Kaledin, L. A.; Komissarov, A. V.; Heaven, M. C. Electronic Spectroscopy and Ionization Potential of UO₂ in the Gas Phase. *J. Phys. Chem.* **2004**, *120*, 5155–5163.
58. Gagliardi, L.; Heaven, M. C.; Krogh, J. W.; Roos, B. O. The Electronic Spectrum of the UO₂ Molecule. *J. Am. Chem. Soc.* **2005**, *127*, 86–91.
59. Goncharov, V.; Kaledin, L. A.; Heaven, M. C. Probing the Electronic Structure of UO⁺ with High-Resolution Photoelectron Spectroscopy. *J. Chem. Phys.* **2006**, *125*, 133202.
60. Heaven, M. C. Probing Actinide Electronic Structure using Fluorescence and Multi-Photon Ionization Spectroscopy. *Phys. Chem. Chem. Phys.* **2006**, *8*, 4497–4509.

61. Merritt, J. M.; Han, J.; Heaven, M. C. Spectroscopy of the UO_2^+ Cation and the Delayed Ionization of UO_2 . *J. Chem. Phys.* **2008**, *128*, 084304.
62. Groenewold, G. S.; Gianotto, A. K.; Cossel, K. C.; Van Stipdonk, M. J.; Moore, D. T.; Polfer, N.; Oomens, J.; de Jong, W. A.; Visscher, L. Vibrational Spectroscopy of Mass Selected $[\text{UO}_2(\text{ligand})_n]^{2+}$ Complexes in the Gas Phase: Comparison with Theory. *J. Am. Chem. Soc.* **2006**, *128*, 4802–4813.
63. Groenewold, G. S.; Oomens, J.; de Jong, W. A.; Gresham, G. L.; McIlwain, M. E.; Van Stipdonk, M. J. Vibrational Spectroscopy of Anionic Nitrate Complexes of UO_2^{2+} and Eu^{3+} Isolated in the Gas Phase. *Phys. Chem. Chem. Phys.* **2008**, *10*, 1192–1202.
64. Groenewold, G. S.; Van Stipdonk, M. J.; Oomens, J.; de Jong, W. A.; Gresham, G. L.; McIlwain, M. E. Vibrational Spectra of Discrete UO_2^{2+} Halide Complexes in the Gas Phase. *Int. J. Mass Spectrom.* **2010**, *297*, 67–75.
65. Groenewold, G. S.; Van Stipdonk, M. J.; Oomens, J.; de Jong, W. A.; McIlwain, M. E. The Gas-Phase Bis-Uranyl Nitrate Complex $[(\text{UO}_2)_2(\text{NO}_3)_5]^-$: Infrared Spectrum and Structure. *Int. J. Mass Spectrom.* **2011**, *308*, 175–180.
66. Ricks, A. M.; Gagliardi, L.; Duncan, M. A. Infrared Spectroscopy of Extreme Coordination: The Carbonyls of U^+ and UO_2^+ . *J. Am. Chem. Soc.* **2010**, *132*, 15905–15907.
67. Ricks, A. M.; Gagliardi, L.; Duncan, M. A. Uranium Oxo and Superoxo Cations Revealed using Infrared Spectroscopy in the Gas Phase. *J. Phys. Chem. Lett.* **2011**, *2*, 1662–1666.
68. Duncan, M. A. Laser Vaporization Cluster Sources. *Rev. Sci. Instrum.* **2012**, *83*, 041101.

69. LaiHing, K.; Taylor, T. G.; Cheng, P. Y.; Willey, K. F.; Peschke, M.; Duncan, M. A. Photodissociation in a Reflectron Time-of-Flight Mass Spectrometer: A Novel MS/MS Scheme for High Mass Systems. *Anal. Chem.* **1989**, *61*, 1458–1460.
70. Cornett, D. S.; Peschke, M.; LaiHing, K.; Cheng, P. Y.; Willey, K. F.; Duncan, M. A. A Reflectron Time-of-Flight Mass Spectrometer for Laser Photodissociation. *Rev. Sci. Instrum.* **1992**, *63*, 2177–2186.
71. Marks, J. H.; Kahn, P.; Vasiliu, M.; Dixon, D.; Duncan, M. A. Photodissociation and Theory to Investigate Uranium Oxide Cluster Cations. *J. Phys. Chem. A* **2020**, *124*, 1940–1953.
72. Frisch, M. J.; Trucks, G. W.; Schlegel, H. B.; Scuseria, G. E.; Robb, M. A.; Cheeseman, J. R.; Scalmani, G.; Barone, V.; Petersson, G. A.; Nakatsuji, H. et al., Gaussian 16, Revision C.01, Gaussian, Inc., Wallingford CT, **2016**.
73. Nakamoto, K. *Infrared and Raman Spectra of Inorganic and Coordination Compounds*, Part B, 5th ed.; John Wiley and Sons: New York, **1997**.
74. de Jong, W. A.; Harrison, R. J.; Nichols, J. A.; Dixon, D. A. Fully Relativistic Correlated Benchmark Results for Uranyl and a Critical Look at Relativistic Effective Core Potentials for Uranium. *Theor. Chem. Acc.* **2001**, *107*, 22–26.
75. Gutowski, K. E.; Cocalia, V. A.; Griffin, S. T.; Bridges, N. J.; Dixon, D. A.; Rogers, R. D. Interactions of 1-Methylimidazole with $\text{UO}_2(\text{CH}_3\text{CO}_2)_2$ and $\text{UO}_2(\text{NO}_3)_2$: Structural, Spectroscopic, and Theoretical Evidence for Imidazole Binding to the Uranyl Ion. *J. Am. Chem. Soc.* **2007**, *129*, 526–536.

76. Wacker, J. N.; Vasiliu, M.; Huang, K.; Baumbach, R. E.; Bertke, J. A.; Dixon, D. A.; Knope, K. E. Uranium(IV) Chloride Complexes: UCl_6^{2-} and an Unprecedented $\text{U}(\text{H}_2\text{O})_4\text{Cl}^4$ Structural Unit. *Inorg. Chem.* **2017**, *56*, 9772–9780.
77. Fang, Z. T.; Garner, E. B.; Dixon, D. A.; Gong, Y.; Andrews, L.; Liebov, B. Laser-Ablated U Atom Reactions with CN_2 to Form UNC, $\text{U}(\text{NC})_2$, and $\text{U}(\text{NC})_2$: Matrix Infrared Spectra and Quantum Chemical Calculations. *J. Phys. Chem. A* **2018**, *122*, 516–528.
78. Adeyiga, O.; Suleiman, O.; Dandu, N. K.; Odoh, S. O. Ground-State Actinide Chemistry with Scalar-Relativistic Multiconfiguration Pair-Density Functional Theory. *J. Chem. Phys.* **2019**, *151*, 134102.
79. Qiu, J.; Burns, P. C. Clusters of Actinides with Oxide, Peroxide or Hydroxide Bridges. *Chem. Rev.* **2013**, *113*, 1097–1120.
80. Wang, X.; Qiu, R. Z.; Long, Z.; Lu, L.; Hu, Y.; Liu, K. Z.; Zhang, P. C. Chemical State of U in U–N–O Ternary System from First-Principles Calculations. *J. Phys. Chem. C* **2019**, *123*, 17155–17162.
81. Denning, R. G. Electronic Structure and Bonding in Actinyl Ions and their Analogs. *J. Phys. Chem. A* **2007**, *111*, 4125–4143.
82. Anderson, N. H.; Xie, J.; Ray, D.; Zeller, M.; Gagliardi, L.; Bart, S. C. Elucidating Bonding Preferences in Tetrakis(Imido)Uranate(VI) Dianions. *Nature Chem.* **2017**, *9*, 850–855.

Table 1. Relative energies of isomers of $U^+(N_2)_n$ for $n = 1-8$ and bond dissociation energies (BDE) calculated for one N_2 ligand or as an average over all N_2 ligands. All energies are listed in kcal/mol. Only the lowest energy spin states of selected isomers are presented here. Isomers indicated with an asterisk contain a NUN^+ core ion.

Isomer	Rel. Energy	BDE last N_2	Mean BDE per N_2
1a sextet	+0.0	13.1	13.1
1b doublet*	+11.9	13.0	13.0
1c sextet	+14.2	-1.1	-1.1
2a sextet	+0.0	10.2	11.6
2b sextet	+0.3	9.8	11.5
2c sextet	+3.0	7.2	10.1
2d doublet*	+9.4	12.7	12.9
3a sextet	+0.0	10.8	11.4
3b sextet	+3.2	10.6	10.3
3c sextet	+4.1	9.7	10.0
3d doublet*	+8.3	11.9	12.5
4a sextet	+0.0	14.0	12.0
4b sextet	+1.6	12.4	11.6
4c sextet	+4.1	9.9	11.0
4f doublet*	+13.0	9.3	11.7
5a sextet	+0.0	13.1	12.2
5b sextet	+1.7	11.4	11.9
5c sextet	+8.0	10.3	10.6
5f doublet*	+16.6	9.5	11.3
6a sextet	+0.0	10.4	11.9
6b sextet	+0.1	10.3	11.9
6c sextet	+1.2	10.9	11.7
6g doublet*	+19.3	7.7	10.7
7a sextet	+0.0	10.4	11.7
7b sextet	+13.8	9.7	7.0
7c sextet	+20.0	4.9	8.9
7d doublet*	+30.1	-0.4	9.1
8a sextet	+0.0	8.7	11.3
8b sextet	+18.5	4.0	9.0
8c sextet	+18.7	3.7	9.0

*contains NUN^+

FIGURE CAPTIONS

Figure 1. Mass spectrum obtained using a pure N₂ expansion and laser vaporization of a depleted uranium metal rod. Complexes of U⁺(N₂)_n are found to be relatively intense only for n = 1–8. A large decrease in intensity observed for n > 8 may indicate that U⁺(N₂)₈ is the fully coordinated complex.

Figure 2. Photodissociation of U⁺(N₂)_n for n = 8 measured with excitation at 355 and 532 nm (Nd:YAG harmonics) and infrared at 2212 cm⁻¹. The ratio of the photon energy to the number of N₂ molecules eliminated is consistent at both 355 and 532 nm, indicating an average U⁺-N₂ bond energy of 12 kcal/mol. Photodissociation at 2212 cm⁻¹ is likely a multiphoton process.

Figure 3. Infrared photodissociation spectra of U⁺(N₂)_n for n = 3–8 in the N₂ stretching region. The position of the normally infrared inactive N₂ stretch is marked with the red dashed line.

Figure 4. The lowest energy structures of U⁺(N₂)_n for each value of n. These structures are all in the sextet spin state which was found to be the lowest in energy for all U⁺(N₂)_n isomers. The n = 4 and 5 structures have trigonal bipyramidal coordination, while the n = 6, 7, and 8 complexes successively build toward a square-prism structure.

Figure 5. The experimental spectrum of U⁺(N₂)₃ with simulated spectra for the lowest energy isomer, 3a, in its sextet, quartet and doublet states. The lower traces display the simulated spectra for isomers 3b, 3c, and 3d in their sextet spin state. Side-on bonding (isomer 3c) and

NUN⁺ formation (isomer 3d) are predicted to yield spectra closer to the bands observed, but these isomers are predicted to lie higher in energy than the 3a isomer.

Figure 6. The experimental spectrum of U⁺(N₂)₄ with simulated spectra of isomers 4a, 4b, and 4c sextets, as well as those for isomers 4d (side-on bonding) and 4f (NUN⁺ core ion). No predicted spectrum provides a satisfactory match with the experiment.

Figure 7. The experimental spectrum of U⁺(N₂)₆ compared to spectra simulated for different structural isomers and spin states.

Figure 8. The experimental spectrum of U⁺(N₂)₈ with simulated spectra for isomers 8a, 8b, and 8c sextets. The predicted band position for the cubic isomer 8a is close to the observed peak, while the less-symmetric isomers would be predicted to yield more complex spectra.

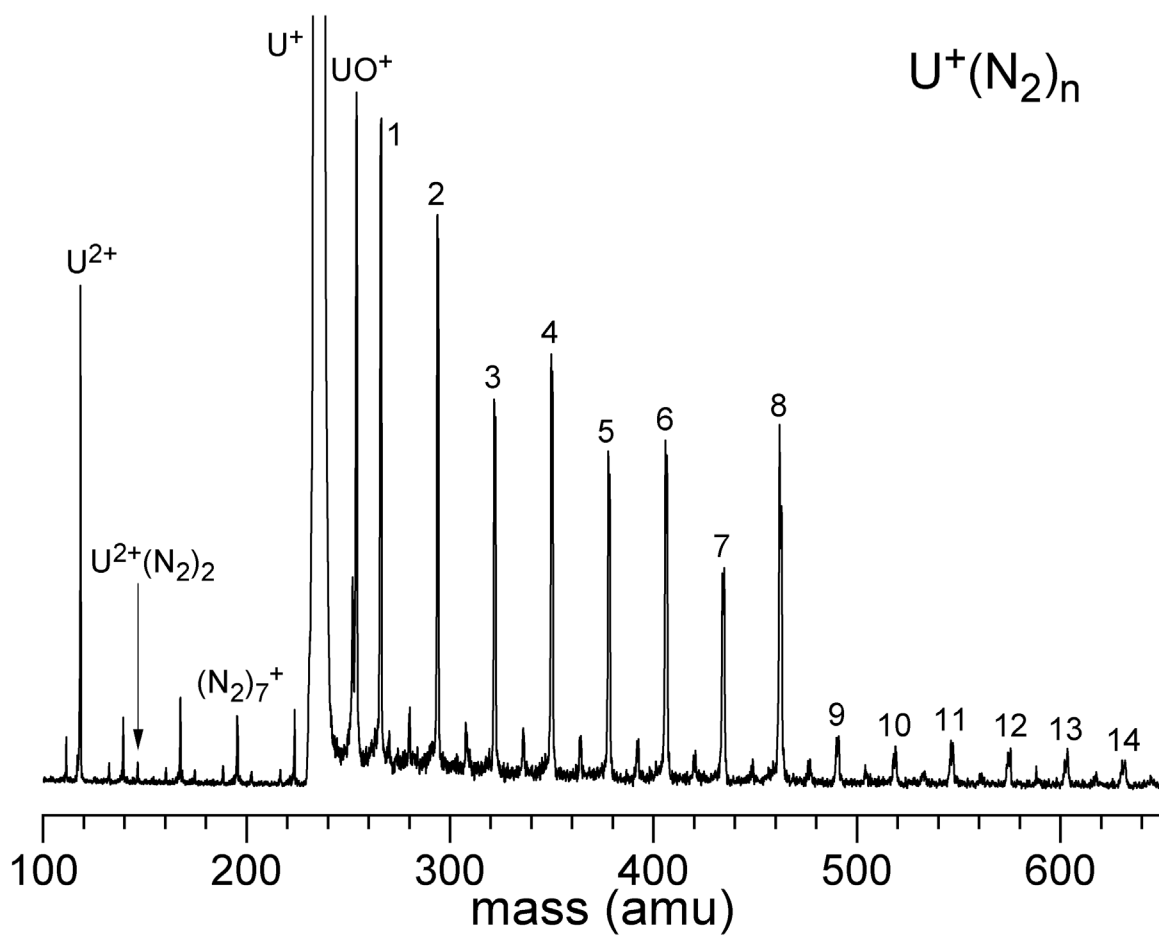


Figure 1.

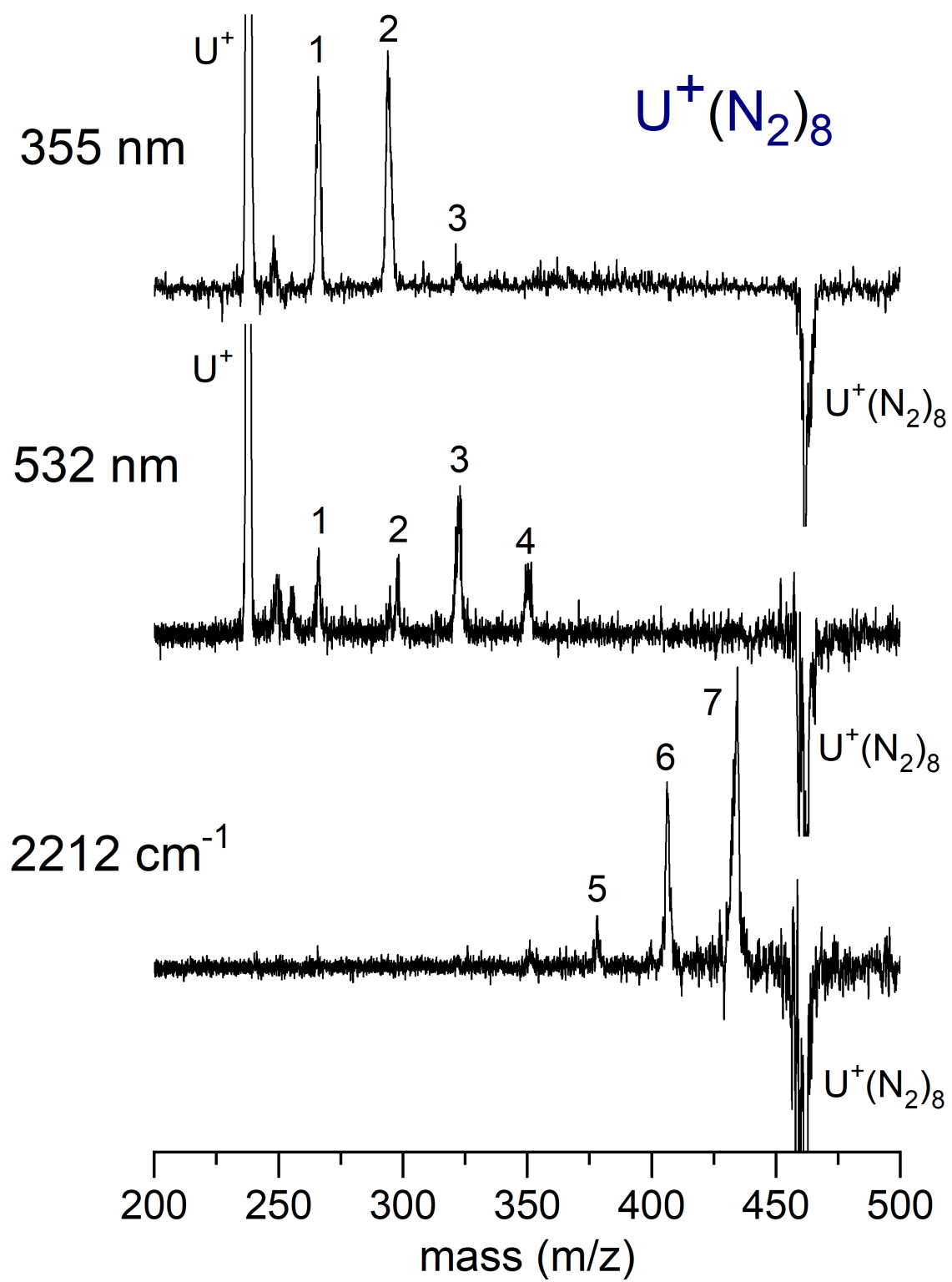


Figure 2.

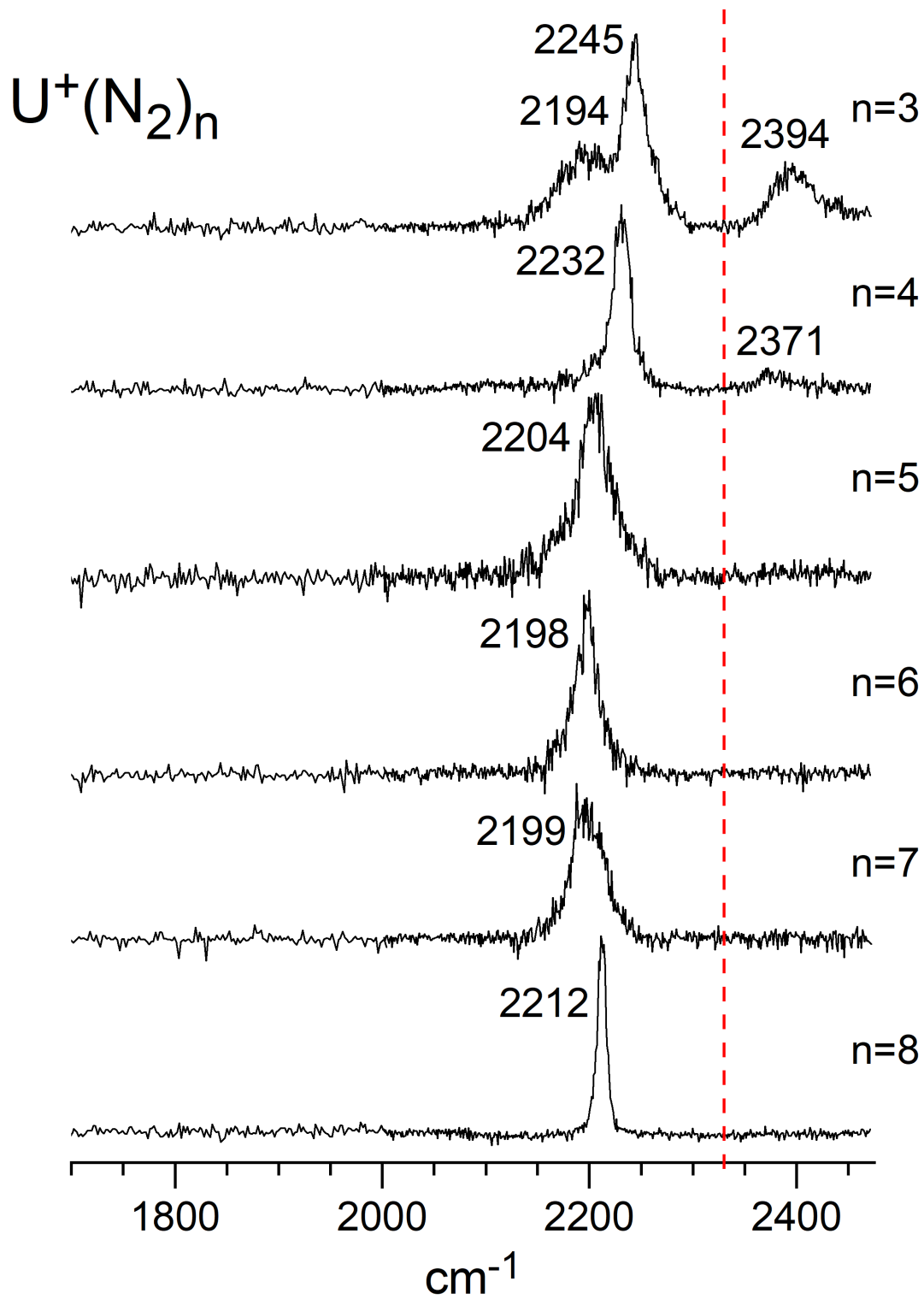


Figure 3.

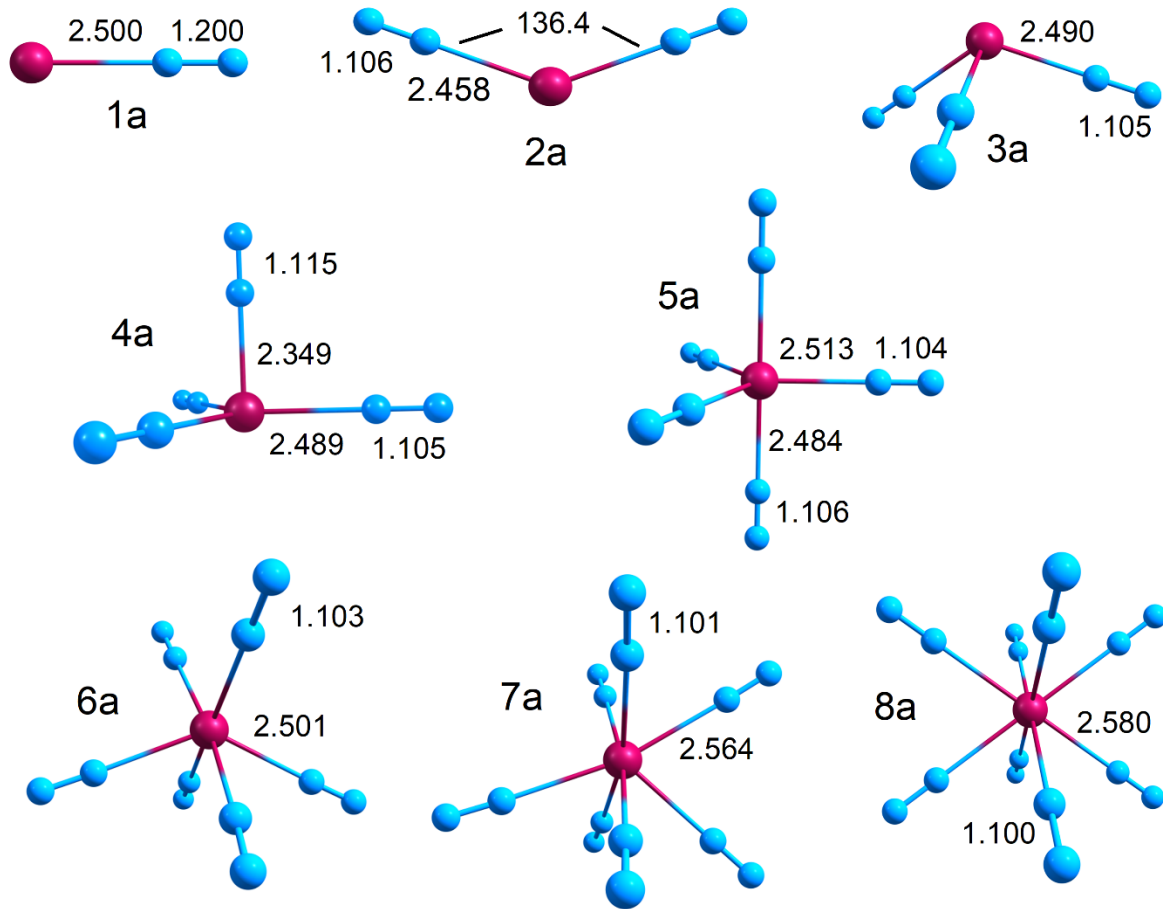


Figure 4.

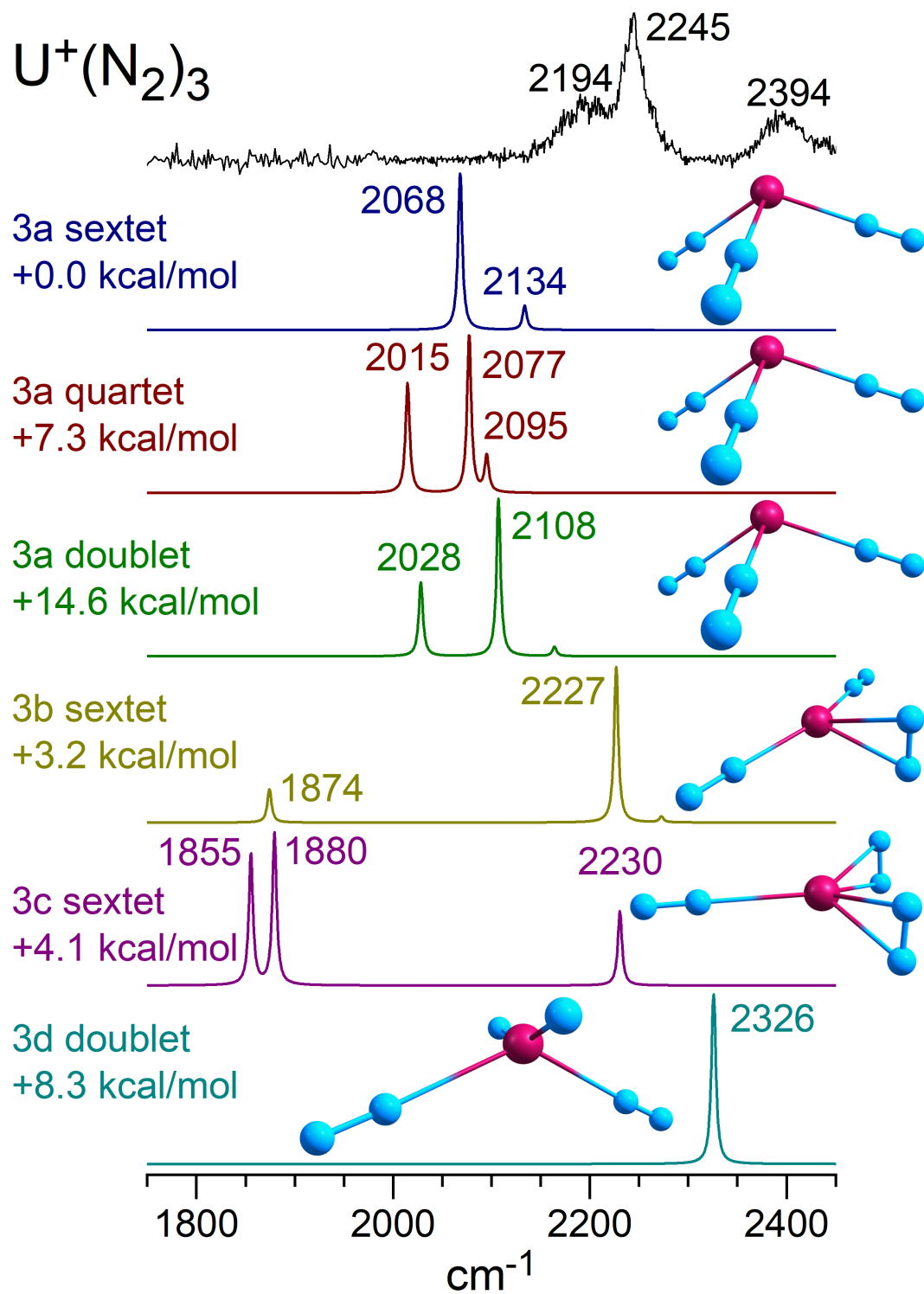


Figure 5.

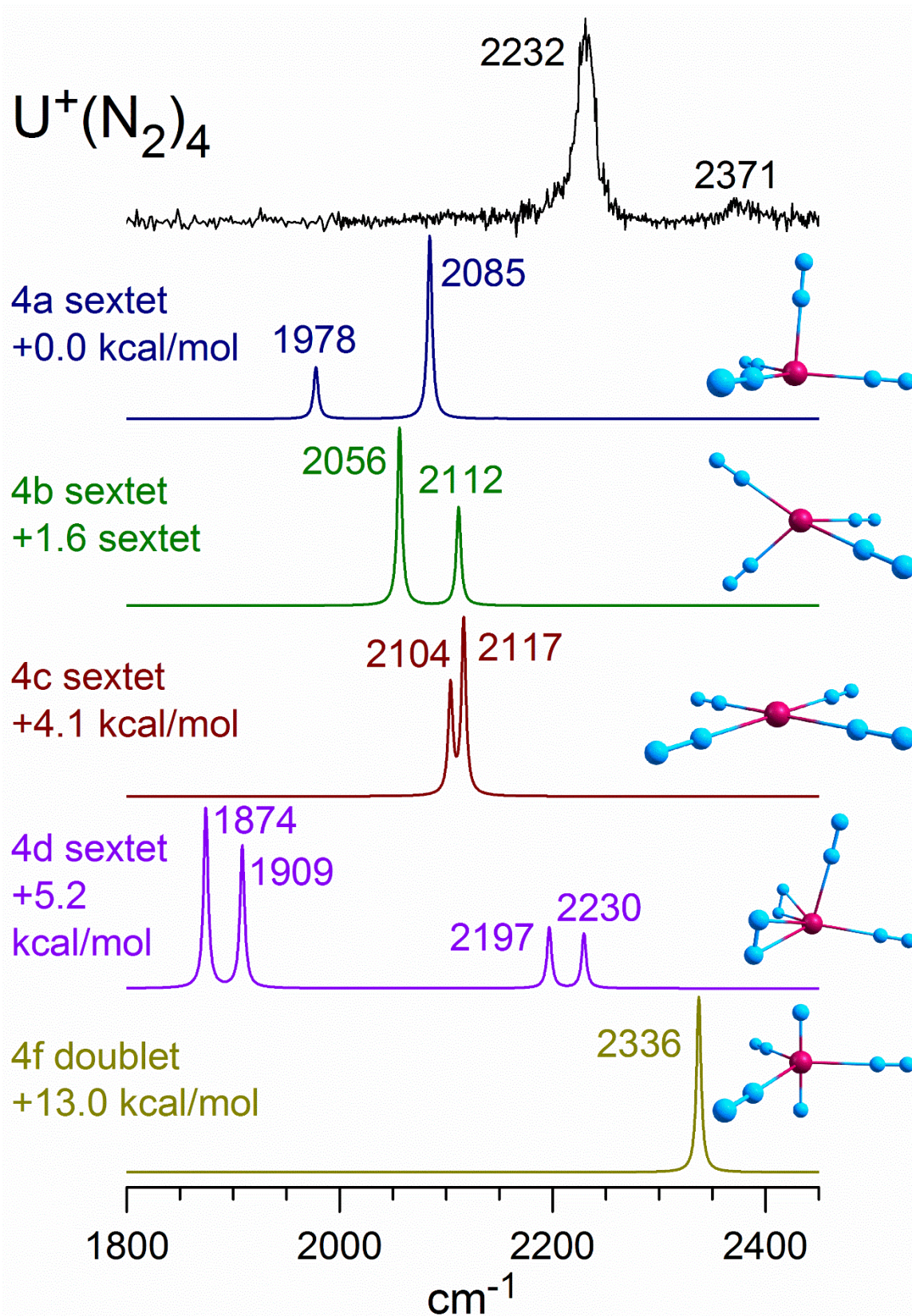


Figure 6.

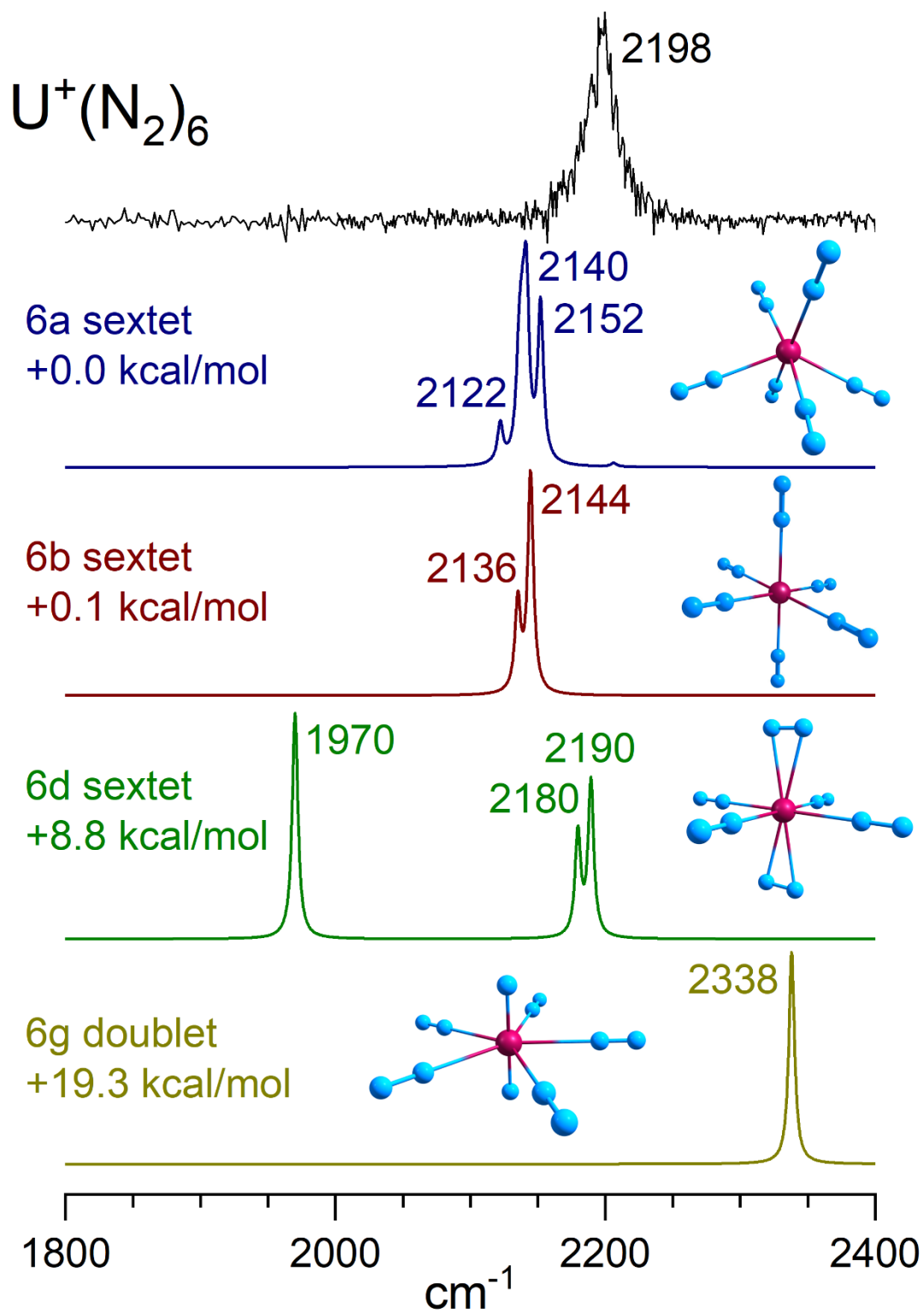


Figure 7.

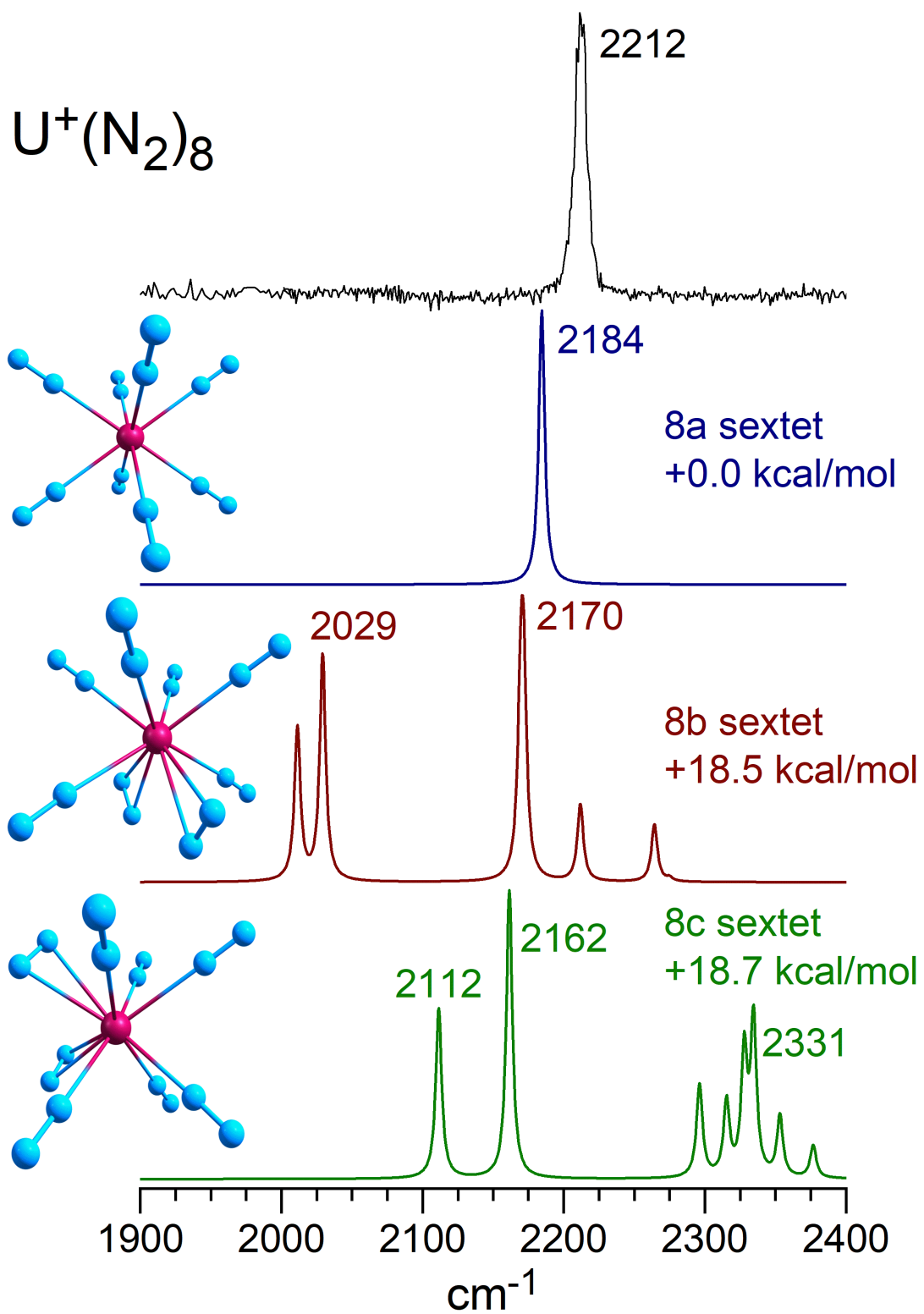


Figure 8.

ToC Graphic:

